Procedia Manufacturing

Volume 1, 2015, Pages 696–707

43rd Proceedings of the North American Manufacturing Research Institution of SME http://www.sme.org/namrc

In-Process Tool Flank Wear Estimation in Machining Gamma-Prime Strengthened Alloys Using Kalman Filter

Farbod Akhavan Niaki*, Durul Ulutan, and Laine Mears

Clemson University – International Center for Automotive Research, Greenville, S.C., U.S.A.

fakhava@clemson.edu, dulutan@clemson.edu, mears@clemson.edu

Abstract

Monitoring tool wear in machining processes is one of the critical factors in reducing downtime and maximizing profitability and productivity. A worn out tool can deteriorate the surface finish or dimensional accuracy of the part. Due to the uncertainties that originate from machining, workpiece material composition, and measurement, predicting tool wear is a challenging task in modern manufacturing processes. Low cost sensing technology for measuring spindle current is commonly deployed in the CNC machine to measure spindle power consumption for predicting tool wear. In this study, spindle power information was integrated into a Kalman filter methodology to predict tool flank wear in cutting hard-to-machine gamma-prime strengthened alloys. Results show a maximum of 18% error in estimation, which indicates a good potential of using Kalman filter in predicting tool flank wear.

Keywords: low cost manufacturing, spindle power, tool wear, Kalman filter

1 Introduction

Tool Condition Monitoring (TCM) is gaining more attention in automated manufacturing processes in recent times (Yen *et al.*, 2004). 20% of machining downtime is reported to be due to tool wear, which causes surface deterioration and can be detrimental to machine health (Vallejo *et al.*, 2005). The history of studying tool wear goes back almost a half century, and various models have been proposed to measure tool wear that can be categorized into two major classes: Offline (direct) methods and online (indirect) methods.

Offline methods of tool wear measurement require direct access to the process that needs to be interrupted: The machine is stopped, and the tool is taken out of the machine for measurement using a pre-installed device (Ertunc *et al.*, 2001). Because of direct measurement of tool wear, these methods

* Corresponding Author

Peer-review under responsibility of the NAMRI Scientific Committee

doi:10.1016/j.promfg.2015.09.018

are relatively more accurate for tool wear monitoring, but impractical in automated manufacturing systems due to the tedious nature of the required work. In addition, when the whole process is stopped, machining downtime is increased and the rate of productivity is decreased. Optical microscope and vision systems are two examples of measurement devices that have been used in the literature (Jeon and Kim, 1988; Pedersen, 1990).

An alternative for offline methods of studying tool wear is online methods, which require measuring external signals such as Acoustic Emission (AE), machining forces, spindle power consumption, and vibration, and relating them to tool wear (Cuppini *et al.*, 1990; Li, 2002; Lin and Yang, 1995; Wang *et al.*, 2002). The advantage of online methods over offline methods is that there is no need to interrupt the process, so online methods can be incorporated in automated machining processes without the loss of productivity. The main disadvantage is the existence of noise in signals, which requires some additional signal processing for extracting the related features of the signal to relate to tool wear. Another challenge is to find a suitable model for estimation. There are various models proposed by researchers which are categorized as (*i*) empirical models that characterize tool wear through running multiple experiments in different cutting conditions and fitting an appropriate function (Li, 2002), (*ii*) mechanistic models that relate cutting force or power through mechanically derived equation to tool wear (Cuppini *et al.*, 1990; Fu *et al.*, 1984; Xu *et al.*, 2011), and (*iii*) dynamic models that characterize the progress of tool wear in state space time series (Danai and Ulsoy, 1987a; Danai and Ulsoy, 1987b).

Recently, tool wear studies in frequency and time-frequency domains gained some attention. Machine learning techniques such as Neural Network have been widely used by researchers to predict tool wear (Wang *et al.*, 2002; Xu *et al.*, 2011). Support Vector Method (SVM), Hidden Markov Model (HMM), and Self-Organizing Map (SOM) are some other methods that have been used for predicting or categorizing tool wear in various machining processes such as drilling, micro-milling, and milling (Ertunc *et al.*, 2001; Owsley *et al.*, 1997; Zhu *et al.*, 2009). Kalman filter is another method that shows good noise suppression characteristic and it has been used by some researchers in machining process control (Möhring *et al.*, 2010).

The objective of this study is improving the tool wear estimation using low cost sensing technology in machining hard to machine alloys. Accurate estimation of tool wear is of great importance in automated machining processes because of decreasing machining idle time and improving productivity. The organization of this work is as follows: theoretical background of Kalman filter and proper mechanistic model are discussed in section 2. In section 3, the experimental setup is explained and selected cutting conditions for experiments are given. The proper method for identifying state noise covariance, measurement noise covariance and initial estimations for Kalman filter are explained in section 4. Results and conclusions are provided in sections 5 and 6.

2 Theoretical Background

2.1 Kalman Filter

Bayesian estimation was introduced by Thomas Bayes who proposed the basic formulation, known as the Bayes rule, in the 18th century (Hoff, 2009). According to this rule, the probability of an event x (*i.e.* $p(x|y)$) can be derived by multiplying the initial (*i.e. a priori*) belief of x (*i.e.* $p(x)$) with the observed data set $p(y|x)$, and dividing by the marginal distribution of observed data $p(y)$. This marginal distribution $p(y)$ can be derived as shown in Eq. (1).

$$p(y) = \int p(y \mid x)\, p(x) dx \tag{1}$$

Bayesian estimation is extensively used in the context of data mining where batches of observations (*i.e.* measurements) are available to estimate state x. Rudolf Kálmán coined a recursive estimation method in 1960 (Kalman filter), which estimates the states of a system at each time step and updates the estimation when a new measurement is available (Kalman, 1960). Since then, the Kalman filter has been widely used in the area of target tracking and navigation, where a linear behavior of system is valid. The Extended Kalman filter (EKF) and unscented Kalman filter (UKF) are also proposed for tracking states in nonlinear systems (Haykin, 2001). For state estimation of x, Kalman filter uses a discrete linear state space equation (Eq. 2):

$$x_k = Ax_{k-1} + Bu_{k-1} + w_{k-1} \tag{2}$$

where k shows the time step, A is a matrix that relates the states at the previous time step (k-1) to the current time step (k), B is a matrix that relates inputs u at the previous time step to the current states, and w is the noise (uncertainty) for state estimation. This noise is assumed to have a normal distribution with zero mean and covariance Q (Eq. 3). The measurement equation is described as a discrete stochastic model that relates current state to measured signals (Eq. 4), where z_k is the measured signal, H is a matrix that relates current states of system to the most recent measurements and v_k is the measurement noise which is assumed to have a normal distribution with zero mean and covariance R.

$$w_k \sim N(0, Q) \tag{3}$$

$$z_k = Hx_k + v_k \tag{4}$$

Kalman filter starts with *a priori* at time k, which is updated based on the previous knowledge at time k-1. As soon as the measurements become available, *a priori* will be updated to find *a posteriori* of states. The first update in the algorithm to find *a priori* is called time update and the second update to find *a posteriori* is called measurement update. Because the process is recursive, there is no need to wait for the batch of measurements to be available. Time and measurement updates are described as below:

(1) Time update:

$$\hat{x}_k^- = A_{k-1}\hat{x}_{k-1} + Bu_{k-1} \tag{5}$$

$$P_k^- = A_{k-1}P_{k-1}A_{k-1}^T + Q_{k-1} \tag{6}$$

(2) Measurement update:

$$K_k = P_{k-1}^- H_k^T (H_k P_{k-1}^- H_k^T + R_k)^{-1} \tag{7}$$

$$\hat{x}_k = \hat{x}_k^- + K_k(z_k - H_k\hat{x}_k^-) \tag{8}$$

$$P_k' = (I - K_k H_k)P_k^- \tag{9}$$

where P_k^- is *a priori* error covariance of states, P_k' is *a posteriori* error covariance of states, $\hat{x}_k^-$ is *a priori* estimation of states, $\hat{x}_k$ is *a posteriori* estimation of states and K_k is the Kalman gain derived by minimizing the *a posteriori* error covariance, and R_k is the measurement error covariance (Haykin, 2001).

2.2 Mechanistic Tool Wear Model

It was shown by researchers that the tangential component of the machining force in milling can be formulated as Eq. (10), where K' and c are constants, $\bar{h}$ is the mean chip thickness, a_p is the depth of cut, f is the feedrate, φ is the instantaneous angle of rotation and F_t is tangential force. (Altintas and Yellowley, 1989).

$$F_t = K'\bar{h}^c a_p f \sin\varphi \tag{10}$$

Unlike turning where the uncut chip thickness h can be considered constant, milling induces changing chip thickness with angle of rotation so that h can be written as a function of the rotational angle, using Figure 1 as schematic of milling. Then, the mean chip thickness $\bar{h}$ can be written in terms of the entrance and exit immersion angles (ψ_1 and ψ_2, respectively) as shown in Eq. (11). In conventional milling tests, these two angles are usually constant, so Eq. (11) reduces to Eq. (12), where C_1 is a constant.

$$\bar{h} = \frac{1}{\psi_1 + \psi_2}\int_{\varphi_{in}}^{\varphi_{out}} h(\varphi) = \frac{f}{\psi_1 + \psi_2}(\sin\psi_1 + \sin\psi_2) \tag{11}$$

$$\bar{h} = C_1 f \tag{12}$$

It was shown that with an increase in tool wear, the magnitude of force increases as well (Choudhury and Rath, 2000). It was shown that the change in magnitude of tangential force F_t^{wear} is a function of the material hardness H_h, the friction coefficient μ, the tool flank wear VB (Waldorf *et al.*, 1992), and the tool wear length s represented by Eq. (13), where s is assumed to be equal to the depth of cut a_p (Shao *et al.*, 2004). All the parameters in Eq. (13) can be assumed constant in milling except for VB, which changes relative to the volume of material removed in the process. Then, adding Eq. (13) to Eq. (10), the resultant tangential force can be written as Eq. (14), where C_2 is a constant that summarizes the constant variables in Eq. (13).

$$F_t^{wear} = \mu VBH_h s \tag{13}$$

$$F_t = K'C_1 f^{c+1} a_p \sin\varphi + C_2 VB \tag{14}$$

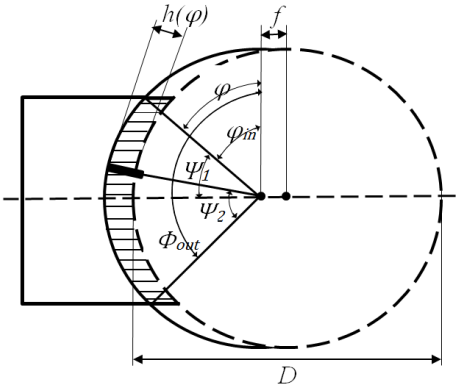

Figure 1: Milling Schematic (Shao *et al.*, 2004)

It was also shown by (Waldorf *et al.*, 1992) that the constant K' is dependent on cutting conditions including feedrate, and depth of cut (Eq. 15), where C_3 is a constant, and α_1 and α_2 are the feedrate and

depth of cut exponents, respectively. Plugging Eq. (15) into Eq. (14), the tangential force is derived as a function of cutting conditions (Eq. 16). Multiplying the tangential force F_t with the cutter diameter D and spindle speed N yields to instantaneous cutting power P shown in Eq. (17).

$$K' = C_3 f^{\alpha_1} a_p^{\alpha_2} \tag{15}$$

$$F_t = C_1 C_3 f^{c+\alpha_1+1} a_p^{\alpha_2+1} \sin\varphi + C_2 VB \tag{16}$$

$$P = C_1 C_3 D f^{c+\alpha_1+1} N a_p^{\alpha_2+1} \sin\varphi + C_2 DNVB \tag{17}$$

Note that the average power can be simply determined by integrating Eq. (17) from entering angle to exiting angle of the block. Assuming constant depth of cut, spindle speed and feedrate, average power is simplified as:

$$P = K_1 + K_2 VB \tag{18}$$

3 Experimental Setup

Rene-108 (R-108) was chosen to explore the performance Kalman filter for in-process estimation of tool wear. An OKUMA GENOS M460-VE 3-axis CNC machine was used to end mill (in down-milling direction) rectangular blocks of size 60 x 80 x 25 mm, using a water-soluble coolant. A 2-flute indexable tool holder with a diameter of 15.875 mm was used, and the width of cut was chosen to be 9.5 mm that corresponds to 60% tool engagement, as this was the maximum manufacturer recommendation for the particular tool holder. Full length of the blocks (60 mm) was utilized for machining, which was considered as a "pass". At the chosen width of cut, 24 tests were conducted on the block: 8 tests with 3 replications. Depth of cut, cutting velocity and feedrate for each pass are kept constant at 0.5 mm, 25 m/min and 0.1 mm/rev respectively. The cutting conditions are determined based on the industrial applications targeted by this study, and keeping the cutting conditions constant is due to the fact that a change in the cutting conditions can induce abrupt changes in the behavior of hard-to-machine alloys. Therefore, in order to duplicate the same machining conditions as in industrial applications, these conditions were kept constant. A data acquisition device (DAQ) was programmed to capture the spindle power consumption while cutting with high sampling rate. To measure spindle power in high sampling frequency, the output of the TMAC transducer (Figure 2) was fed into the NI9215 analog input module mounted on NI-cRIO9103 chassis programmed with LabVIEW. Data was collected in voltage at sampling frequency of 10.24 kHz.

Inserts used in this work were Sandvik Coromill (R390-11 T3 08M-PM 1030). The 1030 grade (TiAlN PVD coated) is recommended by Sandvik for milling R-108 due to its resistance to material build-up on the cutting edge and plastic deformation (Sandvik, 2006). Fresh unworn inserts were used at the beginning of each set of tests which contain 8 passes. Taking out the insert from tool holder for measurement and installing it back can induce additional error due to the radial and axial insert run outs. To avoid taking out the inserts, tool holder was taken out of the machine and flank wear on the bottom edge of insert was measured using an Olympus optical microscope and average flank wear was calculated. The progress of tool flank wear is shown on Figure 3 for test 1.2, 1.4, 1.6 and 1.8 (first replication). Spindle power consumption was measured for each pass. The mean value of cutting power in the 42-48 mm cutting distance was selected as the average cutting power affected by tool flank wear at each test, since this region typically is reflective of the peak value of power consumption with worn tool. In Figure 4, an exemplified description of the spindle cutting power is shown for test 1.3. Measured power and tool flank wear for all the tests are shown in Table 1.

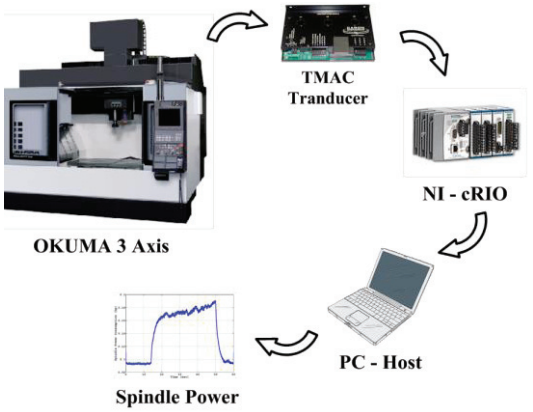

Figure 2: Data Acquisition with NI-cRIO9103

Table 1: Spindle power and flank wear measurement

Replication 1			Replication 2			Replication 3		
Test #	*P* (10^{-3} hp)	*VB* (μm)	Test #	*P* (10^{-3} hp)	*VB* (μm)	Test #	*P* (10^{-3} hp)	*VB* (μm)
1.1	29	84	2.1	32	83	3.1	32	81
1.2	32	89	2.2	36	87	3.2	33	87
1.3	24	100	2.3	38	103	3.3	35	99
1.4	33	108	2.4	37	107	3.4	34	103
1.5	36	111	2.5	44	109	3.5	39	109
1.6	41	116	2.6	30	116	3.6	38	115
1.7	37	119	2.7	41	125	3.7	36	116
1.8	36	125	2.8	44	127	3.8	42	120

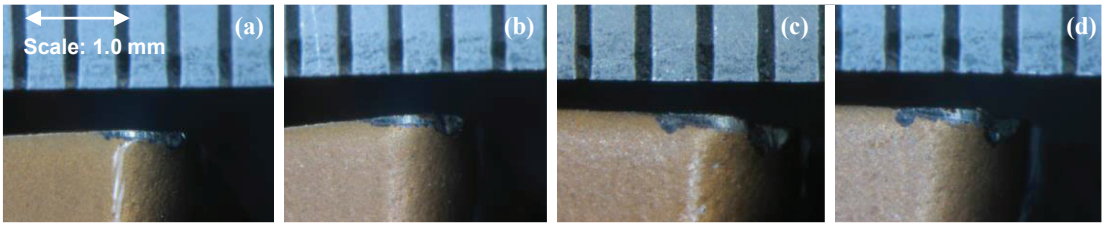

Figure 3: Measured flank wear for (a) Test 1.2, (b) Test 1.4, (c) Test 1.6, (d) Test 1.8

4 Stochastic Modeling of Tool Flank Wear

The dynamic behavior of tool wear is nonlinear at the initial stages, linear at intermediate stages, and nonlinear at the final stages before catastrophic failure (Koren *et al.*, 1991). Due to the high strength and hardness of R-108, the progress of tool wear was relatively fast, and the first stages of tool wear were not captured while testing. Hence, tool wear progress was considered as a linear function of volume of material removed (*MR*) while machining.

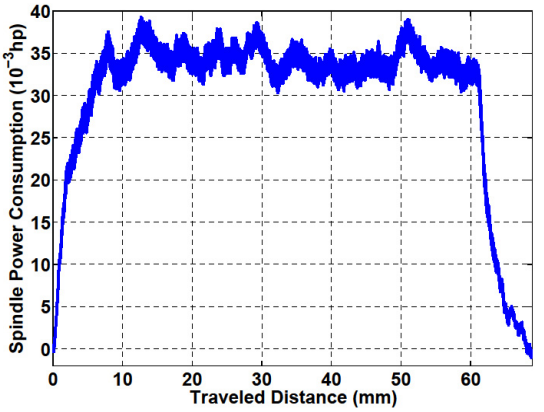

Figure 4: Cutting power for Test 1.3

Linear regression was used to find the slope of tool wear curves for each replication of tests as shown in Figure 5. R^2_{adj} values of 96%, 94%, and 95% for the three replications of the tests validate the aforementioned linear tool wear assumptions.

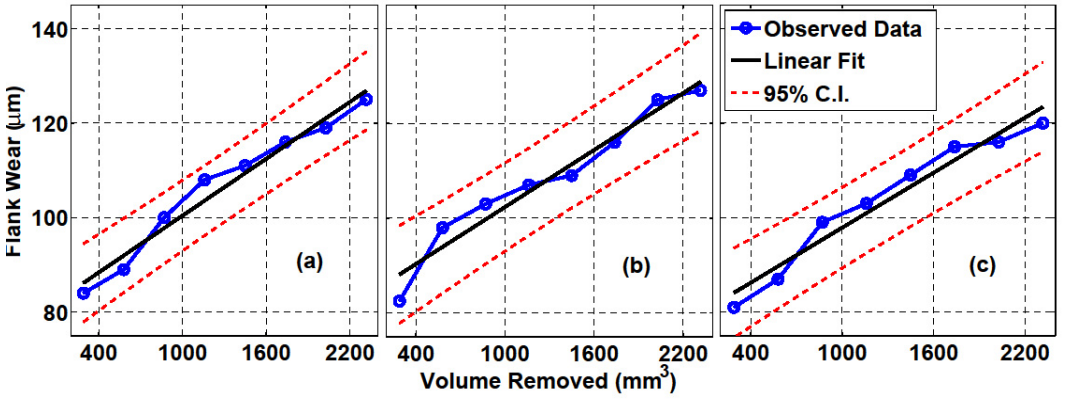

Figure 5: Linear regression results of (a) replication 1 (b) replication 2, and (c) replication 3

Considering a linear region for tool wear and assuming flank wear and slope of tool wear growth (VB') as the states of the system, discretized state space equation can be written as Eq. (19), where Δt is the time-step size, which is constant and equivalent to the volume of removed material (MR). Because the cutting conditions are kept constant in this work, VB' can be defined as Eq. (20).

$$\frac{VB(k)-VB(k-1)}{\Delta t} = VB'(k) \rightarrow VB(k) = VB(k-1) + VB'(k)\Delta t \tag{19}$$

$$VB'(k) = VB'(k-1) \tag{20}$$

The state error should be added to Eq. (19) and Eq. (20) as normally distributed noise. Note that error variances for tool wear and tool wear rate are assumed to be independent of each other. The stochastic state space equation is described in matrix format in Eq. (21-22).

$$\begin{bmatrix} VB(k) \\ VB'(k) \end{bmatrix} = \begin{bmatrix} 1 & MR \\ 0 & 1 \end{bmatrix} \begin{bmatrix} VB(k-1) \\ VB'(k-1) \end{bmatrix} + \begin{bmatrix} w_1(k) & 0 \\ 0 & w_2(k) \end{bmatrix} \quad (21)$$

$$\begin{bmatrix} w_1(k) \\ w_2(k) \end{bmatrix} \sim N\left(\begin{bmatrix} 0 \\ 0 \end{bmatrix}, \begin{bmatrix} Q_1 & 0 \\ 0 & Q_2 \end{bmatrix} \right) \quad (22)$$

The variance Q_1=13 μm^2 was calculated based on the maximum variance in tool flank wear measurements between replications of tests. The variance Q_2 = 1.4×10^{-7} μm^2/mm^6 was calculated as the variance between slopes of linear regression curves. Using Eq. (18), a linear relation was considered between the observed signal (*i.e.* spindle power consumption) and tool flank wear when cutting conditions are constant.

A linear regression is used for each set of tests as shown in Figure 6, and average values for K_1 and K_2 were calculated. The measurement error covariance was calculated the same way as Q_1. The value of K_1, K_2 and the measurement noise variance R are 13.1 hp, 0.22 hp/μm and 18.7 hp^2, respectively. Note that, it is possible to tune the measurement error covariance based on the performance of the filter. By decreasing R, the effect of *a priori* will strengthen on the estimations. Eq. (18) can be written in discrete format to run the Kalman filter as given in Eq. (23), where the measurement error $v(k)$ can be defined as a normal distribution with zero mean and R variance.

$$\Delta P(k) = C_2 VB(k) + v(k) \quad (23)$$

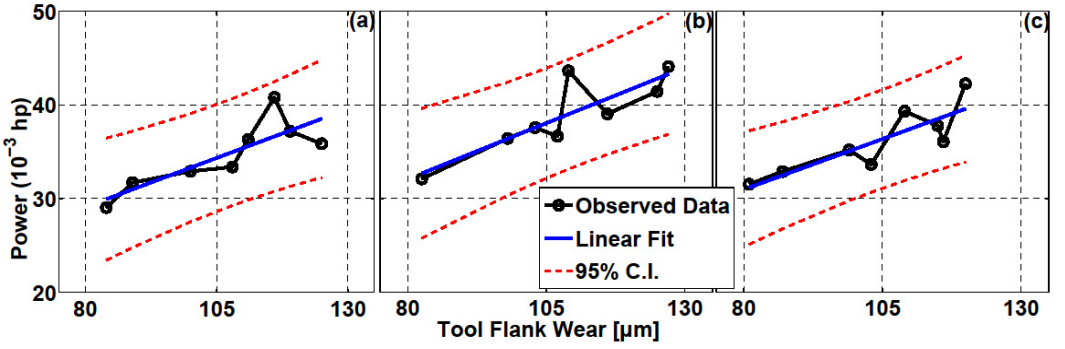

Figure 6: Linear fit of spindle power vs. flank wear for (a) replication 1, (b) replication 2, and (c) replication 3

To run the Kalman filter, an initial point and an initial covariance for states are required. The initial point (x_0) was calculated simply as the mean of predicted flank wear from test 1.1, 2.1, and 3.1. To find the initial error of the flank wear, the error between the mean of measured flank wear for first tests of each replication which appears as expected value of $VB_{i,1}$ in Eq. (24) and estimated flank wear based on measured power which appears as expected value of $\Delta P_{i,1}/C_2$ was calculated. The error of flank wear rate was calculated as the difference between the slope of measured flank wear (first term in Eq. (25)) and predicted flank wear using tests 1 and 2 for each replication (second term in Eq. (25)). Combining these two errors together and using Eq. (26), the initial error covariance of tool wear and tool wear was calculated as 1.74 μm and 130.2 μm^2/mm^3.

$$e_0 = E(VB_{i,1}) - E(\frac{\Delta P_{i,1}}{C_2}) \; i \in \{1,2,3\} \quad (24)$$

$$e_0' = E(\frac{VB_{i,1} - VB_{i,2}}{MR}) - E(\frac{P_{i,1} - P_{i,2}}{C_2 MR}) \; i \in \{1,2,3\} \quad (25)$$

$$P_0 = \begin{bmatrix} e_0 & e_0' \end{bmatrix} \begin{bmatrix} e_0 \\ e_0' \end{bmatrix} = \begin{bmatrix} e_0^2 & e_0 e_0' \\ e_0 e_0' & e_0'^2 \end{bmatrix} \quad (26)$$

5 Results

The results of the tool flank wear estimation and the corresponding 95% confidence intervals calculated from the estimated covariance (P_{cov}) are shown in Figure 7. Note that, measurement error covariance (R) was tuned to get the least relative error between the estimation and measurements. The least error was observed in replications 1 and 3. However, it was observed that the Kalman filter estimated tool flank wear with relatively constant error in replication 2, where the maximum error was observed at 18%. The average percent error of estimation for each replication is 5.4, 9.4 and 4.8% respectively. As shown in Figure 7, Kalman filter performed with less than 20% estimation error when cutting power is used as the measurement signal; it is able to suppress the fluctuation of measured spindle power. However, the filter was unable to estimate relatively smooth flank wear growth.

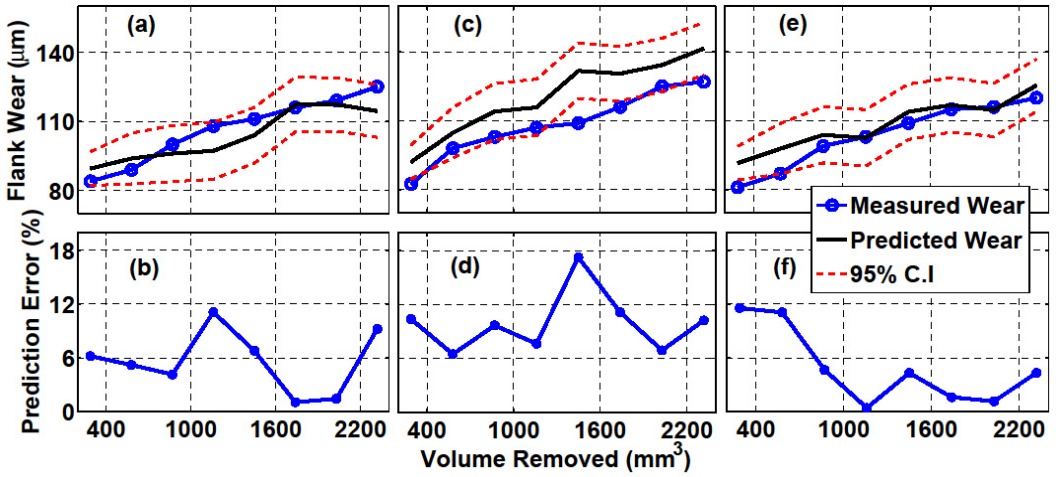

Figure 7: Flank wear estimation and its error for (a&b) Test Series 1, (c&d) Test Series 2, (e&f) Test Series 3

The comparison of tool flank wear estimation with and without the Kalman filter is shown in Figure 8. The black line represents the predicted flank wear based on deterministic equation (*i.e.* linear equation relating flank wear to consumed spindle power). The red dashed line represents the Kalman filter estimation. It was observed that the Kalman filter was able to compensate the offset between the deterministic estimation and the actual measurement. To quantify the performance of the Kalman filter and the deterministic approach, Root Mean Square Error (RMSE) of each method was calculated and compared in Table 2. Kalman filter reduced the RMSE 41% for the 1st replication, and 25% for the 3rd replication; however, a slight increase in the error was observed for the 2nd replication. This can be due to several factors such as radial or axial run out error that is uncontrollable and may happen when installing the insert, and subsurface damage (smearing of grains along the direction of cut) which increases work hardening of the block (Figure 9). Moreover, linear model is assumed for the process and implemented in Kalman filter framework (Eq. 18), but tool wear is a complex non-stationary dynamic process and linear models may not fully represent the complex dynamics of tool wear. Measurement error (*i.e.* high signal to noise ratio) in power signal and human induced error while measuring tool wear with microscope are other sources of error.

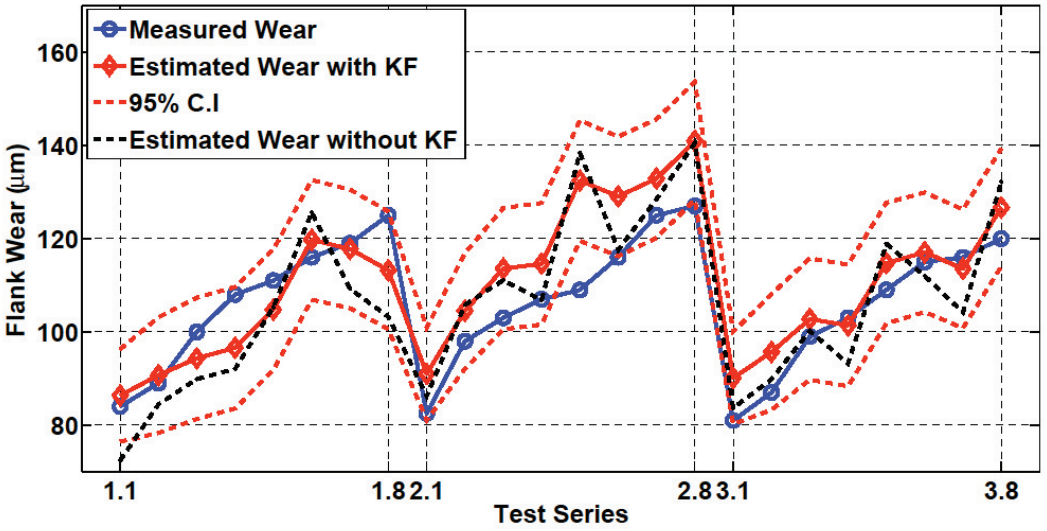

Figure 8: Comparison of estimated flank wear with and without use of Kalman filter to actual measurement

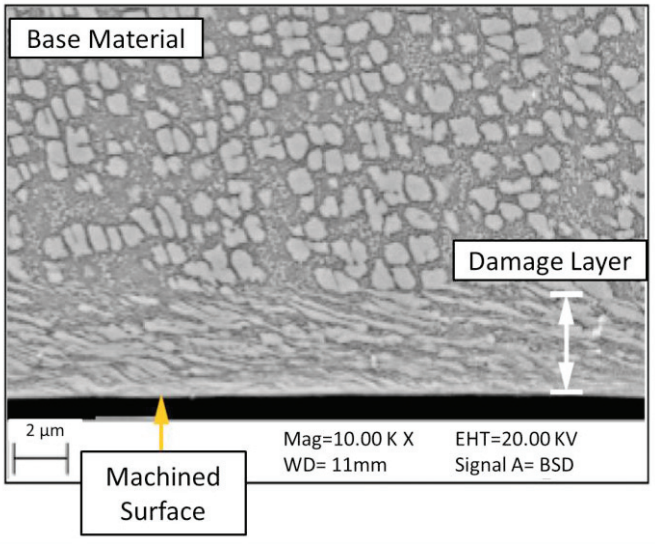

Figure 9: Subsurface damage due to machining

Table 2: Comparison of the stochastic and deterministic estimations

Replication	RMSE(µm) deterministic	RMSE (µm) Kalman filter	Change (%)
1	12	7	-41
2	12	13	+8
3	8	6	-25

6 Conclusions

In this study, an adaptive tool flank wear estimation method was proposed in end milling of gamma-prime strengthened alloys. Tracking tool wear in modern manufacturing processes is critical due to the fact that it can reduce downtime of the machine and increase productivity simultaneously. Spindle power consumption was used as the observed signal due to the low cost and easy implementation of Eddy current sensors in CNC machines. The main conclusions of this study are given as below:

- A discrete linear model of mechanistic tool wear was formulated to be used with Kalman filter. A design of experiment with relatively mild cutting conditions was used along with high frequency DAQ system to capture spindle power consumption.
- Proper variances of state and measurement error were identified and the Kalman filter was tuned to have the least possible error in estimation. It was shown that the Kalman filter can predict tool flank wear with a maximum average error of 10%. The performances of the Kalman filter and the deterministic estimation were compared and it was shown that the Kalman filter could estimate tool wear with 7, 13 and 6% RMSE in replications 1-3. Low estimation error is beneficial in automated machining process where proper action should be taken before catastrophic tool failure occurs.

To increase the performance of estimation, more experiments with different cutting conditions can be used. Furthermore, other signals such as cutting force and vibration can be fused with spindle cutting power, and nonlinear models that better capture the dynamic behavior of tool wear can be used instead of the linear models for relating flank wear to observed signal.

Acknowledgments

The authors wish to thank the National Science Foundation for support of this work under Grant No. 0954318. Any opinions, findings, and conclusions or recommendations expressed in this material are those of the authors and do not necessarily reflect the views of the National Science Foundation.

References

Altintas Y and Yellowley I. In-process detection of tool failure in milling using cutting force models. *Journal of Manufacturing Science and Engineering* 1989; 111(2): 149-157.

Choudhury S and Rath S. In-process tool wear estimation in milling using cutting force model. *Journal of Materials Processing Technology* 2000*;* 99(1): 113-119.

Cuppini D, D'errico G and Rutelli G. Tool wear monitoring based on cutting power measurement. *Wear* 1990*;* 139(2): 303-311.

Danai K and Ulsoy AG. An adaptive observer for on-line tool wear estimation in turning, part I: Theory. *Mechanical Systems and Signal Processing* 1987*;* 1(2): 211-225.

Danai K and Ulsoy AG. An adaptive observer for on-line tool wear estimation in turning, part II: Results. *Mechanical Systems and Signal Processing* 1987; 1(2): 227-240.

Ertunc HM, Loparo KA and Ocak H. Tool wear condition monitoring in drilling operations using hidden markov models (HMMs). *International Journal of Machine Tools and Manufacture* 2001; 41(9): 1363-1384.

Fu HJ, DeVor RE and Kapoor SG. A mechanistic model for the prediction of the force system in face milling operations. *Journal of Manufacturing Science and Engineering* 1984; 106(1): 81-88.

Haykin SS. *Kalman filtering and neural networks*. Wiley Online Library, 2001.

Hoff PD. *A first course in bayesian statistical methods*. Springer, 2009.

Jeon J and Kim S. Optical flank wear monitoring of cutting tools by image processing. *Wear* 1988; 127(2): 207-217.

Kalman RE. A new approach to linear filtering and prediction problems. *Journal of Fluids Engineering* 1960; 82(1): 35-45.

Koren Y, Ko T, Ulsoy AG and Danai K. Flank wear estimation under varying cutting conditions. *Journal of Dynamic Systems, Measurement, and Control* 1991; 113(2): 300-307.

Li X. A brief review: Acoustic emission method for tool wear monitoring during turning. *International Journal of Machine Tools and Manufacture* 2002; 42(2): 157-165.

Lin S and Yang R. Force-based model for tool wear monitoring in face milling. *International Journal of Machine Tools and Manufacture* 1995; 35(9): 1201-1211.

Möhring H, Litwinski K and Gümmer O. Process monitoring with sensory machine tool components. *CIRP Annals-Manufacturing Technology* 2010; 59(1): 383-386.

Owsley LM, Atlas LE and Bernard GD. Self-organizing feature maps and hidden markov models for machine-tool monitoring. *IEEE Transactions on Signal Processing* 1997; 45(11): 2787-2798.

Pedersen KB. Wear measurement of cutting tools by computer vision. *International Journal of Machine Tools and Manufacture* 1990; 30(1): 131-139.

Sandvik, C. *Steel milling stars, GC4240 and GC1030, C-1140, A pair of grades that won't crack under pressure* 2006.

Shao H, Wang HL and Zhao XM. A cutting power model for tool wear monitoring in milling. *International Journal of Machine Tools and Manufacture* 2004; 44(14): 1503-1509.

Vallejo AG, Nolazco-Flores J, Morales-Menendez R, Sucar LE and Rodriguez CA. Tool-wear monitoring based on continuous hidden markov models. *Progress in pattern recognition, image analysis and applications* 2005; Springer Berlin Heidelberg.

Waldorf DJ, Kapoor SG and Devor RE. Automatic recognition of tool wear on a face mill using a mechanistic modeling approach. *Wear* 1992; 157(2): 305-323.

Wang L, Mehrabi MG and Kannatey-Asibu E. Hidden markov model-based tool wear monitoring in turning. *Journal of Manufacturing Science and Engineering* 2002; 124(3): 651-658.

Xu C, Xu T, Zhu Q and Zhang H. Study of adaptive model parameter estimation for milling tool wear. *Strojniški Vestnik-Journal of Mechanical Engineering* 2011; 57(7-8): 568-578.

Yen Y, Söhner J, Lilly B and Altan T. Estimation of tool wear in orthogonal cutting using the finite element analysis. *Journal of Materials Processing Technology* 2004; 146(1): 82-91.

Zhu K, Wong YS and Hong GS. Multi-category micro-milling tool wear monitoring with continuous hidden markov models. *Mechanical Systems and Signal Processing* 2009; 23(2): 547-560.